Data-Driven Linear Parameter-Varying Modeling and Control of Flexible Loads for Grid Services

Preprint

Yue Chen and Andrey Bernstein

National Renewable Energy Laboratory

Presented at the 2020 American Control Conference (ACC)
July 1–3, 2020

NREL is a national laboratory of the U.S. Department of Energy
Office of Energy Efficiency & Renewable Energy
Operated by the Alliance for Sustainable Energy, LLC

This report is available at no cost from the National Renewable Energy Laboratory (NREL) at www.nrel.gov/publications.

Contract No. DE-AC36-08GO28308

Conference Paper
NREL/CP-5D00-76334
July 2020

Data-Driven Linear Parameter-Varying Modeling and Control of Flexible Loads for Grid Services

Preprint

Yue Chen and Andrey Bernstein

National Renewable Energy Laboratory

Suggested Citation
Chen, Yue, and Andrey Bernstein. 2020. *Data-Driven Linear Parameter-Varying Modeling and Control of Flexible Loads for Grid Services: Preprint*. Golden, CO: National Renewable Energy Laboratory. NREL/CP-5D00-76334.
https://www.nrel.gov/docs/fy20osti/76334.pdf.

Conference Paper
NREL/CP-5D00-76334
July 2020

National Renewable Energy Laboratory
15013 Denver West Parkway
Golden, CO 80401
303-275-3000 • www.nrel.gov

NOTICE

This work was authored in part by the National Renewable Energy Laboratory, operated by Alliance for Sustainable Energy, LLC, for the U.S. Department of Energy (DOE) under Contract No. DE-AC36-08GO28308. This work was supported by the Laboratory Directed Research and Development (LDRD) Program at NREL. The views expressed herein do not necessarily represent the views of the DOE or the U.S. Government.

Cover Photos by Dennis Schroeder: (clockwise, left to right) NREL 51934, NREL 45897, NREL 42160, NREL 45891, NREL 48097, NREL 46526.

Data-Driven Linear Parameter-Varying Modeling and Control of Flexible Loads for Grid Services

Yue Chen, Andrey Bernstein

***Abstract*— Flexible loads have great potential to improve the electric grid's flexibility a nd s tability. T o e ffectively control large ensembles of heterogeneous loads, reliable models thereof are required. This paper presents a data-driven modeling and control approach to manage flexible l oads f or p roviding grid services. We leverage a linear parameter-varying autoregressive moving average (LPV-ARMA) model to describe the aggregate load response, where the parameters in the model are used to capture external environmental impacts (e.g., weather). A gain-scheduling feedback controller is then developed to adapt to environmental variations. This data-driven approach can be easily applied to different types of loads in various environmental conditions. In addition to the ensemble controller, distributed load controllers are designed to deliver grid services, while maintaining the quality of service of inherent load tasks. We demonstrate the work on the IEEE 37-node distribution system for real-time power regulation services through control of thermostatically controlled loads.**

I. Introduction

Modern power systems require increased flexibility to adapt to the widespread penetration of volatile renewable energy resources. It has been widely acknowledged that the flexibility i n e lectric l oads c an b e h arnessed t o p rovide grid services. Compared to expensive and limited-lifetime batteries, demand-side loads are more economic and sustainable [1]; however, the performance of demand response is largely restricted by the nature of working patterns of each type of load, and current demand response programs are mainly applied to event-based load shedding services [2].

Extensive work in the literature explores the potential of flexible l oads t o e nhance t he fl exibility an d st ability of power systems [3]–[10]. The main idea is to transform the flexibility f rom l oads t o t he g rid b y s hifting l oad power consumption. Electric loads, such as plug-in electric vehicles (EVs), heating, ventilation, and air conditioning (HVAC) systems, data centers, residential thermostatically controlled loads (TCLs), pool pumps, and agricultural irrigation systems have sufficient fl exibility to su pport an d pr ovide se rvices to the grid.

Y. Chen and A. Bernstein are with the Power Systems Engineering Center, National Renewable Energy Laboratory, Golden, CO 80401, USA {yue.chen, andrey.bernstein}@nrel.gov

Because the contribution from a single load is negligible to the grid (especially for low-power residential loads), it is important to develop aggregate load models that will be used in demand response control schemes. An ensemble of loads can be modeled as a dynamic system whose dynamics depend on the internal load operation physics as well as the external signal that is used to engage them. Most existing works consider or approximate the aggregate system by a linear time-invariant (LTI) model, e.g., [4], [11], [12], where it is assumed that the load working environment is time invariant. LTI systems have attractive properties that make the controller design easier. In many situations, however, the LTI model is not sufficient to capture the load response. As an example, the power consumption of a water heater is largely related to the incoming water temperature.

This paper proposes linear parameter-varying (LPV) modeling and control of the aggregate loads, where the parameters capture the environment variables that affect load behavior. The model is identified using a data-driven approach so that the general framework can be applied to different loads in various environments. The LPV model presents a set of linear approximations for the system with respect to varying parameters. As a result, the standard analysis tools for the LTI systems are still applicable to the LPV system. In this regard, we design a gain-scheduling feedback controller to deal with the variability of the environmental parameters.

In addition to the aggregate controller, local load controllers need careful design to ensure that loads complete their routine operation tasks while providing grid services. The decision-making methods for local controllers can be classified into two categories: centralized methods and distributed methods. The centralized methods usually need full load information to make decisions for each individual load. In contrast, the distributed methods allow each local controller to make its own decision to balance the grid objective and its load quality of service (QoS). It relieves the computation and communications requirements in the centralized methods and protects the local privacy. This paper adopts the distributed approach for local load control. In addition, we employ a randomized policy in the local control to desynchronize load responses.

The proposed hierarchical control architecture is illustrated in Fig. 1. At the upper level, there is a central controller at a utility that receives grid measurements (e.g., frequency, voltage) and computes a control common for flexible loads. At the local level, we propose a parallel distributed control architecture where each load has its own controller. Each local controller is designed to balance the utility's grid

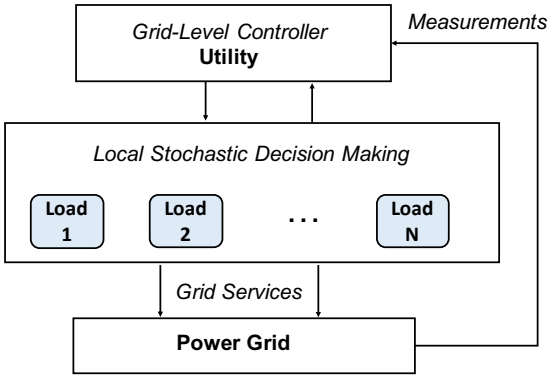

Fig. 1. Schematic diagram of the control architecture.

service and the local objective that maintains the QoS to the load owner. To desynchronize loads and unlock flexibility, a stochastic method is introduced to randomize load behaviors so that two identical loads could arrive at different decisions.

In summary, the contributions of this paper are: 1) we develop an LPV model to capture the aggregate load response through a data-driven approach; 2) we design a gain-scheduling feedback controller based on the developed LPV model; and 3) we develop distributed local controllers to respond to the grid-level controller and maintain its own load QoS within a strict bound.

The rest of the paper is organized as follows. Section II introduces the load QoS metric and proposes a distributed randomized local control. Section III presents the data-driven LPV modeling and control techniques. Section IV presents simulation results on the IEEE 37-node distribution system with 500 residential homes. Section V concludes the paper and discusses future research.

II. Individual Load QoS and Control

Under nominal operation, loads are controlled to complete their routine tasks, e.g., an air conditioner keeps the room temperature within a comfortable range. We use the concept of QoS to represent the load work performance on its routine tasks. Without loss of generality, the QoS for an individual load can be expressed as [5]:

$$Q_t = \sum_{\tau=0}^{T_f} \beta^\tau q(X_{t-\tau}, u_{t-\tau}) \tag{1}$$

$$X_{t+1} = f(X_t, u_t) \tag{2}$$

where X_t represents the load state; u_t is the control signal applied on the load; the function q extracts QoS features from the load state and control; and the QoS is defined as the discounted sum of the q values, in which the discount factor $\beta \in [0,\, 1]$ and T_f defines the moving window size.

With proper selection of T_f, β, and $q(X, u)$, the QoS function Q_t can be designed to represent a broad range of load QoS. For example, if $\beta = 0$ and/or $T_f = 0$ (we use the convention $0^0 = 1$), then $Q_t = q(X_t, u_t)$ can be used to define an instant load QoS, such as the temperature of a TCL. When $T_f > 0$ and $0 < \beta \leq 1$, QoS value Q_t considers historical trajectory of relevant quantities, such as energy consumption and cycling behavior of an on/off load.

Generally, the load QoS is determined by an adjustable setpoint. For example, the cleanliness of a swimming pool is controlled by the setpoint of daily operation time, and the room temperature is maintained by the temperature setpoint of an air conditioner. In this paper, we assume that the load QoS has some level of flexibility, such that $Q_t \in \mathcal{Q}_t$ is considered good QoS. Typically, $\mathcal{Q}_t$ represents a box constraint: $\mathcal{Q}_t = [\underline{Q}_t,\, \bar{Q}_t]$.

Using (1), the constraint $Q_t \in \mathcal{Q}_t$ can be transformed to the control variable $u_t \in \mathcal{U}_t$, such that

$$\mathcal{U}_t := \left\{ u : \sum_{\tau=1}^{T_f} \beta^\tau q(X_{t-\tau}, u_{t-\tau}) + q(f(X_t, u)) \in \mathcal{Q}_t \right\} \tag{3}$$

Thus, each load has its real-time control variable constraints, according to its predefined QoS flexibility.

We propose a randomized control policy to avoid load synchronization. Assuming a load received a control command $\bar{u}_t$ from the grid operator, it is randomized by a uniform distribution:

$$u_t = \mathcal{P}_{\mathcal{U}_t}\{\bar{u}_t(1 + \alpha N_t)\} \tag{4}$$

where $\mathcal{P}_{\mathcal{U}_t}$ is the closest point projection operator that ensures good load QoS; the random variable N_t follows the uniform distribution on $[-1, 1]$; and $\alpha > 0$ is a small constant.

Example: Thermostatically Controlled Loads

This paper considers TCLs as the example to demonstrate the proposed approach. TCLs such as air conditioners, electric water heaters, and refrigerators are the major power consumers in residential households. The power flexibility is extracted from the thermal inertia in TCLs that allows for a slight shift in the power consumption without a noticeable change in the temperature. Under proper control, TCLs are great demand-side resources to improve the grid's flexibility and stability without significant impact on load owners' comfort.

The dynamics for one TCL can be approximated by an RC model [4], [13]:

$$T_{t+1} = aT_t + (1 - a)(T_t^o - m_t R P^{trans}) + w_t \tag{5}$$

where T_t is the object temperature; $a \in (0, 1)$ is the factor of inertia, defined as $a = e^{-\tau/(CR)}$, where $\tau > 0$ is the time step, and C and R are the TCL's thermal capacitance and resistance, respectively; T_t^o is the outdoor temperature; w_t is the modeling noise; and P^{trans} is the TCL's energy transfer rate, which is positive for cooling and negative for heating. The internal control variable m_t equals to 1 when the TCL is ON and 0 when the TCL is OFF. It is defined as follows for a cooling device:

$$m_t = \begin{cases} 0, & T_t < \min(\Omega_t) \\ 1, & T_t > \max(\Omega_t) \\ m_{t-1}, & \text{otherwise} \end{cases}$$

where Ω_t is the TCL's temperature deadband, which is defined by the temperature setpoint T_t^{set} and the deadband width δ as $\Omega_t := [T_t^{set} - \delta/2,\, T_t^{set} + \delta/2]$.

Each TCL has its nominal temperature setpoint that reflects the load owner's preference. We define the QoS function as the deviation from the preferred temperature setpoint $T_\bullet^{set}$:

$$Q_t := T_t^{set} - T_\bullet^{set} \tag{6}$$

A large $|Q_t|$ indicates bad QoS.

In this particular TCL application, we define the control variable the same as the deviation from the nominal QoS setpoint:

$$T_t^{set} := \begin{cases} T_\bullet^{set} - u_t, & \text{for a cooling TCL} \\ T_\bullet^{set} + u_t, & \text{for a heating TCL} \end{cases} \tag{7}$$

The purpose of proposing two different interpretations for the control signal is to ensure all TCLs respond in the same direction towards a given control signal, i.e., a positive (negative) u encourages power consumption (saving).

Based on (6) and (7), we obtain a simple expression for QoS function (1):

$$Q_t = \begin{cases} u_t, & \text{for a cooling TCL} \\ -u_t, & \text{for a heating TCL} \end{cases} \tag{8}$$

Therefore, the load QoS constraint can be easily transformed to the control constraint to restrict the maximal temperature setpoint deviation from the preferred value.

III. LPV System Modeling and Control

In this section, we propose techniques to find an LPV model for the grid-level load response, and we design the controller for grid services. The grid operator needs only a grid-level model that captures the aggregate load response, without detailed individual dynamics. It largely reduces the communications and computation requirements at the central controller. We consider a data-driven approach to identify the load response model so that it can be applied to various types of loads.

To understand the load response over time, the input-output data are collected as a time series. The autoregressive moving average (ARMA) model is a typical tool to model time-series data. For a single-input-single-output system, the ARMA model is given by

$$\begin{aligned} y_t + a_1 y_{t-1} + a_2 y_{t-2} + \cdots + a_m y_{t-m} \\ = b_1 u_{t-1} + b_2 u_{t-2} + \cdots + b_n u_{t-n} \end{aligned} \tag{9}$$

where u_t and y_t are system input and output at t, respectively; and $\{a_1, \dots a_m, b_1, \dots, b_n\}$ are the model coefficients. Here, the control signal u_t is the command sent to flexible loads, e.g., the change in temperature setpoint of air conditioners; the output signal y_t represents the power system outputs, such as the feeder head power and node voltages.

One benefit of using the ARMA model is that it can be easily converted to frequency domain for analysis. By taking the z-transform of (9), we obtain

$$H(z) = \frac{Y(z)}{U(z)} = \frac{b_1 z^{-1} + b_2 z^{-2} + \dots b_n z^{-n}}{1 + a_1 z^{-1} + a_2 z^{-2} + \dots a_m z^{-m}} \tag{10}$$

Because of the environmental variation, however, the ARMA model cannot accurately represent the load response in many situations. To address this issue, the ARMA model is improved to include the impact from the external environment.

A. Linear Parameter-Varying Model

The following proposed method is motivated by [14]. In this paper, we consider multiple environment features and propose coefficient-identification algorithms with a regularization term to prevent model overfitting. For practical applications, we add the data normalization process so that model coefficients are "fairly" treated.

Consider the following parameter-varying ARMA model

$$\begin{aligned} y_t + a_1(\boldsymbol{p}) y_{t-1} + a_2(\boldsymbol{p}) y_{t-2} + \cdots + a_m(\boldsymbol{p}) y_{t-m} \\ = b_1(\boldsymbol{p}) u_{t-1} + b_2(\boldsymbol{p}) u_{t-2} + \cdots + b_n(\boldsymbol{p}) u_{t-n} + \eta_t \end{aligned} \tag{11}$$

where η_t is the modeling error; the vector $\boldsymbol{p} \in \mathbb{R}^v$ collects v environmental features, and

$$\begin{aligned} a_i(\boldsymbol{p}) &:= a_{i,0} + a_{i,1} p_1 + \cdots + a_{i,v} p_v, \text{ for } i = 1, \dots, m \\ b_i(\boldsymbol{p}) &:= b_{i,0} + b_{i,1} p_1 + \cdots + b_{i,v} p_v, \text{ for } i = 1, \dots, n \end{aligned}$$

The model (11) can be represented by a standard linear regression form:

$$\hat{y}_t = \theta^T \phi_{t-1} \tag{12}$$

where $\hat{y}_t$ is the estimate of system output; the matrix θ collects all model coefficients to be identified; the vector ϕ collects input-output data and environmental feature values. The detailed representations of θ and ϕ can be found in appendix.

Consider the loss function that penalizes the modeling error and the L_2 regularization term (standard ridge regression):

$$J(\theta) = \frac{1}{N} \sum_{t=1}^{N} \frac{1}{2} (y_t - \hat{y}_t)^2 + \frac{\lambda}{2} ||\theta||_2^2 \tag{13}$$

where λ is a weighting factor. It is not hard to find the gradient

$$\nabla J(\theta) = \frac{1}{N} \sum_{t=1}^{N} (y_t - \theta^T \phi_{t-1})(-\phi_{t-1}) + \lambda \theta.$$

Setting the gradient to zero, we obtain the least-square solution:

$$\theta = \left[\frac{1}{N} \bar{\phi} \bar{\phi}^T + \lambda I \right]^{-1} \frac{1}{N} \bar{\phi} \bar{y} \tag{14}$$

where $\bar{\phi} = [\phi_0,\, \phi_1, \dots, \phi_{N-1}]$ and $\bar{y} = [y_1,\, y_2, \dots, y_N]^T$.

Online Algorithm. For some applications, especially when the system process is nonstationary, it is useful to update the

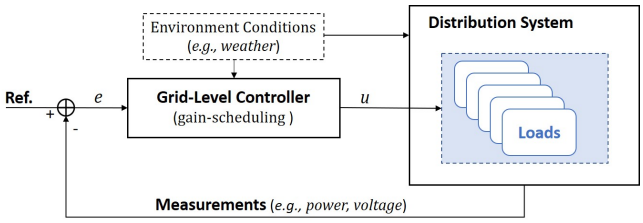

Fig. 2. Schematic of gain-scheduling feedback control.

model in an online fashion. Consider the loss function (13) in one time step:

$$J_t = \frac{1}{2}(y_t - \hat{y}_t)^2 + \frac{\gamma}{2}||\theta||_2^2 \tag{15}$$

We obtain its gradient:

$$\nabla J_t = -(y_t - \hat{y}_t)\phi_{t-1} + \gamma\theta_{t-1}$$

It motivates the following online stochastic gradient descent algorithm:

$$\begin{aligned} e_t =& y_t - \theta_{t-1}^T \phi_{t-1} \\ \theta_t =& (1 - \alpha\gamma)\theta_{t-1} + \alpha e_t \phi_{t-1} \end{aligned}$$

This algorithm is also known as the on-line ridge regression.

Data Normalization. Because the environmental variables are collected in different units with different ranges, data normalization is required to ensure that all features are weighted equally in the model identification. Typical normalization techniques include centering, min-max scaling, standardization, and other transformations [15]. In many applications, normalization also improves the running time of data-driven optimization algorithms.

B. Gain-Scheduling Feedback Control

The LPV-ARMA model (11) can be viewed as a set of LTI approximations with respect to the environmental parameters. For fixed parameters, the model is simply LTI. So the tools for LTI system analysis and controller design are still applicable. Different from fixed controller gains for an LTI system, the gains for an LPV system are adaptable to environmental parameters $\boldsymbol{p}$.

The structure for the gain-scheduling feedback control is given in Fig. 2. Grid services are represented by the reference signal, which is expected to be followed by the distribution system. Based on the error between the reference signal and the system outputs, the controller computes the control signal for loads. We assume that the environmental parameters (such as the weather data) are measurable so that the controller can adjust the gains to adapt to the environment.

In this paper, we apply classic frequency domain techniques (e.g., [16]) to analyze the system and design the controller. For a discrete-time system, the closed-loop transfer function can be expressed in z-domain as

$$H(z, \boldsymbol{p}) = \frac{Y(z, \boldsymbol{p})}{R(z, \boldsymbol{p})} = \frac{C(z, \boldsymbol{p})P(z, \boldsymbol{p})}{1 + C(z, \boldsymbol{p})P(z, \boldsymbol{p})} \tag{16}$$

where $Y(z, \boldsymbol{p})$, $R(z, \boldsymbol{p})$, $C(z, \boldsymbol{p})$, $P(z, \boldsymbol{p})$ are the z-domain representations of the output, reference signal, controller, and system plant, respectively, with respect to the environmental parameter $\boldsymbol{p}$.

It is suggested by (16) that $Y(z, \boldsymbol{p})/R(z, \boldsymbol{p}) \approx 1$ can be achieved by choosing high gains in $C(z, \boldsymbol{p})$; however, the system would become unstable if the gains cross a certain critical point. Note that the closed-loop system (16) has infinite gain when $C(z, \boldsymbol{p})P(z, \boldsymbol{p}) = -1$, which is equivalent to $|C(z, \boldsymbol{p})P(z, \boldsymbol{p})| = 1$ and $\angle C(z, \boldsymbol{p})P(z, \boldsymbol{p}) = -180^o$. Two commonly used stability criteria are the gain margin and phase margin, which define the amount of gain and phase lag that can be increased before instability results.

Therefore, the controller depends on the dynamics of the grid-level loads response $P(z, \boldsymbol{p})$, which is the z-transform of the LPV model (11). The details of LPV modeling and controller design are illustrated in Section IV.

IV. Numerical Demonstration

In this section, we demonstrate the data-driven approach for real-time power regulation through control of TCLs. The numerical results described here are based on simulations of 500 residential households on the balanced IEEE 37-node distribution system [17]. It was observed from the simulation results that a collection of residential TCLs can provide high-quality grid services, with little impact on load QoS.

A. Data Acquisition

We simulated 500 residential households, where each household has an air conditioner, a refrigerator, and a heat pump. In total, $1,500$ TCLs were modeled by (5) with the parameters provided in Table I, where U refers to the uniform distribution. These 500 households were distributed throughout the load nodes in the IEEE 37-node test feeder.

The aggregate load response was modeled using the LPV model (11). Because the air conditioners and heat pumps do not operate at the same time, we developed two different LPV models for hot and cold weather, respectively. For brevity, we show only the LPV modeling and controller design process under hot weather, when air conditioners and refrigerators are engaged. The modeling and control techniques used for cold weather are the same.

To mimic a hot summer environment, we created a 24-hour outdoor temperature profile, as shown on the top in Fig. 3. The corresponding power at the feeder head is plotted on the bottom in Fig. 3. It is found that the feeder head power is closely related with the outdoor temperature because the power is dominated by air conditioners and the contribution from refrigerators is insignificant.

To collect input-output data for system identification, a swept-sine signal (top in Fig. 4) was created to change the TCL temperature setpoints. It allows us to observe the system response to various frequencies of the input signal. Under the same temperature in Fig. 3, the distribution system feeder head power was plotted in the middle of Fig. 4. Its deviation from the nominal power consumption in Fig. 3 was considered as the system output, which is shown on the

TABLE I

TCL PARAMETER VALUES.

Parameter	Air Conditioners	Heat Pumps	Refrigerators
Dead-band width, $\delta(^\circ C)$	$\sim U[0.5\ 1]$	$\sim U[0.5\ 1]$	$\sim U[0.5\ 1]$
Temperature set point, $T^{set}\ (^\circ C)$	$\sim U[23\ 25]$	$\sim U[19\ 21]$	$\sim U[1.7\ 3.3]$
Thermal resistance, $R(^\circ C/\text{kW})$	$\sim U[1.5\ 2.5]$	$\sim U[1.5\ 2.5]$	$\sim U[60\ 80]$
Thermal capacitance, $C(\text{kWh}/^\circ C)$	$\sim U[1.5\ 2.5]$	$\sim U[1.5\ 2.5]$	$\sim U[.05\ 0.15]$
Energy transfer rate, $P^{trans}(\text{kW})$	$\sim U[12\ 16]$	$\sim U[25\ 30]$	$\sim U[0.6\ 0.9]$
Coefficient of performance	2.5	3.5	3

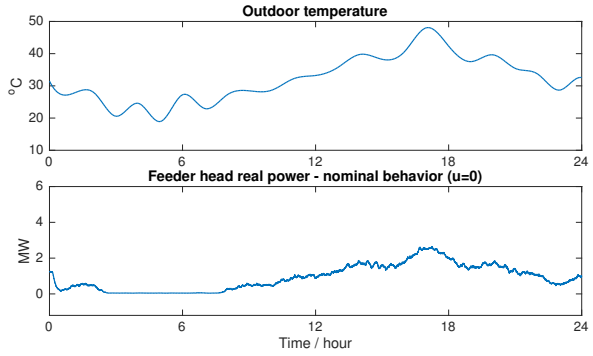

Fig. 3. The outdoor temperature and the nominal feeder head power.

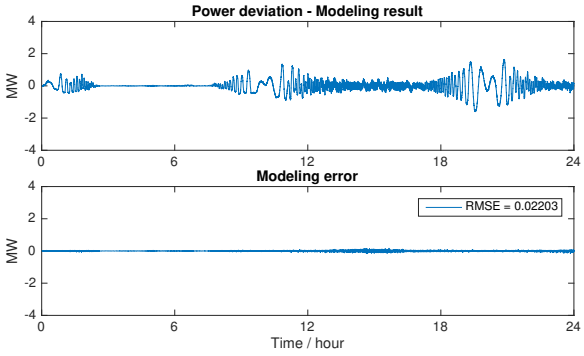

Fig. 5. Modeling result and error.

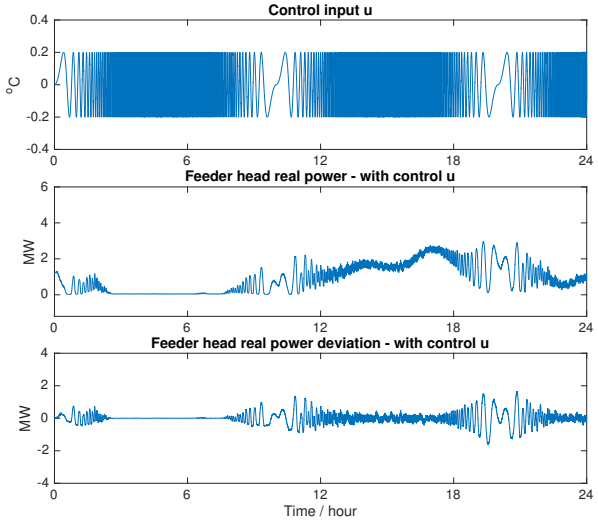

Fig. 4. Feeder head power demand under temperature setpoint control, and its deviation from nominal power in Fig. 3.

bottom in Fig. 4. The goal is to identify the LPV model using input-output simulation data along with the temperature data.

B. System Identification

We used the following two polynomial features:

$$p_{1,t} = \frac{T_t^o - \bar{p}}{\sigma_1}, \quad p_{2,t} = \frac{(T_t^o - \bar{p})^2}{\sigma_2}$$

where T_t^o is the outdoor temperature; $\bar{p} = 20\,^\circ\text{C}$; and σ_1 and σ_2 are standard deviations for the quantities in the numerators, respectively.

A 10-day simulation was performed to collect the input-output data. For brevity, we present only the first 24-hour results in 10 days. The top subplot in Fig. 5 shows the LPV modeling results (11), with modeling orders $m = 31$ and $n = 31$. It closely matches the real system output that shown on the bottom in Fig. 4, and the modeling error is given on the bottom in Fig. 5.

C. Ensemble Controller Design

We designed the controller in the frequency domain. Fig. 7 shows the frequency response of the system with various outdoor temperatures. When the temperature is $25\,^\circ\text{C}$, because most air conditioners are idling, a slight change in the temperature setpoint has little impact on the power consumption. So the response magnitude is very small when the outdoor temperature is $25\,^\circ\text{C}$. As the temperature increases, air conditioners start to actively respond to the temperature setpoint change, and they eventually saturate around $35\,^\circ\text{C}$. The resonant frequencies in these bode plots are in the neighborhood of 5×10^{-2} rad/s, which is consistent with the nominal on-off cycle frequencies of the air conditioners in simulation.

Based on the aggregate load response shown in Fig. 7 and the proposed control structure shown in Fig. 2, we designed the following gain-scheduling PI controller:

$$u_t(T_t^o) = K_p(T_t^o)e_t + K_i(T_t^o)\sum_{\tau=0}^{t} e_\tau \Delta t$$

with proportional and integral gains

$$K_p(T_t^o) = \frac{70 - T_t^o}{50}, \quad K_i(T_t^o) = 0.05K_p(T_t^o)$$

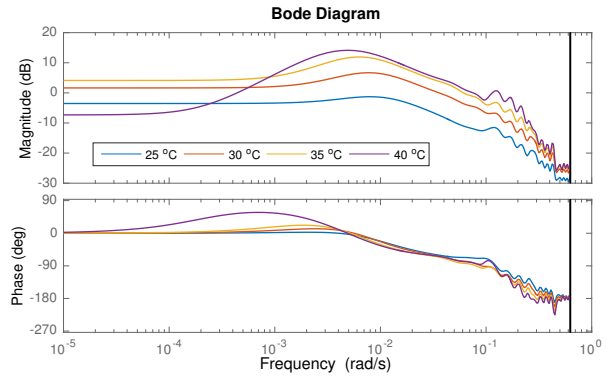

Fig. 7. Frequency response of the feeder head power, driven by the control of TCL temperature setpoint.

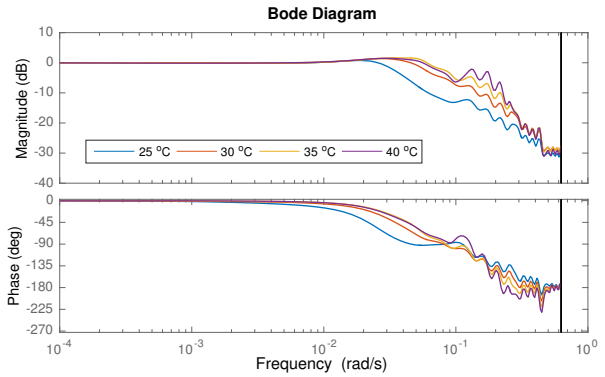

Fig. 8. Frequency response of the closed-loop system, using the gain-scheduling PI control.

where e_t is the error between the reference and the actual system output; $\Delta t = 5$ seconds is the simulation time step; and T_t^o is the outdoor temperature. The controller provides gain margins $\geq$ 10.4 dB and phase margins $\geq$ 52.8° for system stability.

The resulting closed-loop frequency response is presented in Fig. 8. It indicates that these flexible loads can track reference signals of periods as fast as a few minutes.

For the purpose of maintaining good load QoS, we restricted the control signal u within at most 1 °C deviation from the nominal TCL temperature setpoints. In addition, we restricted the integral error e_t^I within predetermined bounds to prevent the integral windup situation in PI control.

D. Grid Service

To illustrate the control performance under a wide range of outdoor temperatures, we created an artificial 48-hour temperature profile that spans $[-20, 40]$ °C to engage all considered TCLs. The temperature is shown on the top in Fig. 6. The left-hand-side (LHS) in Fig. 6 (the first 24-hour period) shows the nominal behavior of the TCLs without control; the right-hand-side (RHS) in Fig. 6 (the second 24-hour period) shows the control performance when the TCLs were controlled to provide the grid service.

Based on the nominal power at the feeder head (on the LHS of Subplot 2 in Fig. 6), we obtain the baseline of 24-hour power, which is shown as the dotted line on RHS of the Subplot 2. The goal is to control the TCLs so that the power deviation from the baseline tracks some reference signal. We consider the regulation signal from the Bonneville Power Administration (BPA) [18] as the reference signal. Because of the capacity limit, the BPA signal was scaled to a proper magnitude that is trackable by the loads. It is shown as the

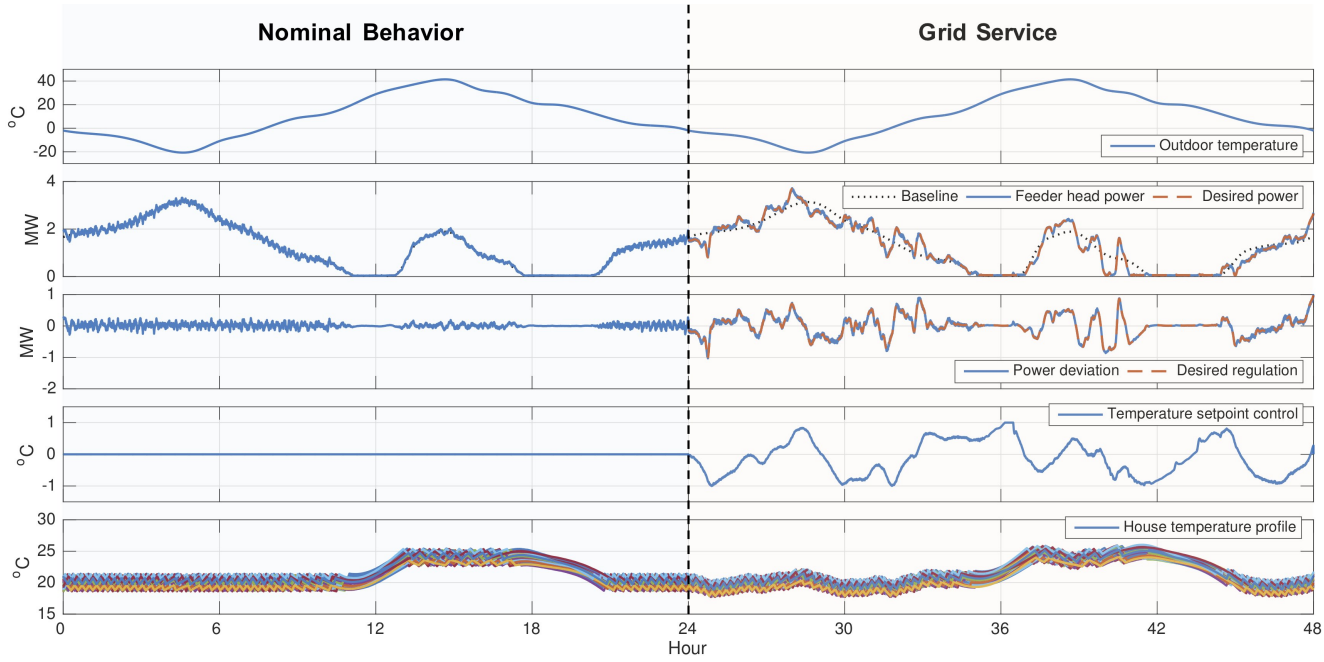

Fig. 6. Control performance of the proposed approach in providing power-balancing grid service through control of the TCL temperature setpoint.

red dashed line on the RHS of Subplot 3 in Fig. 6.

It is found that these TCLs can provide real-time regulation power in the range of $[-1,\ 1]$ MW with power tracking root-mean-square-error (RMSE) of 22 kW (see the RHS of Subplot 3). Considering that the aggregate TCL power is less than 4 MW, the regulation service extracted from these TCLs is significant. In addition, note that the fluctuations that appear in nominal power consumption are also suppressed under the control.

While providing grid service, the impact to home comfort is insignificant because the control signal is restricted to $[-1,\ 1]\,^{\circ}$C. It is verified from the comparison of two 24-hour house temperatures on the bottom in Fig. 6. To conclude, there is a trade-off between the grid service and load QoS: if these TCLs allow more QoS flexibility, a greater regulation service can be provided.

V. Conclusion and Future Work

In this paper, we presented a data-driven LPV modeling and control approach for flexible loads to provide grid services. The approach enables the controller to tune its gains to adapt to changes in the environment. It was demonstrated on the IEEE 37-node distribution system for real-time power regulation service through control of TCLs.

In the future, we plan to extend the application to a wider range of loads that involve more environmental parameters. Other grid services, e.g, voltage regulation, are also of interest for future work. In addition, it is valuable to estimate the grid service capacity from the loads. We aim to estimate the capacity by a similar data-driven approach and use the capacity information for power system planning.

Acknowledgements

We thank Emiliano Dall'Anese (CU Boulder) and Marcello Colombino (ETH) for valuable discussions.

References

[1] N. J. Cammardella, R. W. Moye, Y. Chen, and S. P. Meyn, "An energy storage cost comparison: Li-ion batteries vs distributed load control," in *2018 Clemson University Power Systems Conference (PSC)*, Sep. 2018, pp. 1–6.

[2] "Florida Power and Light: OnCall Program," https://www.fpl.com/save/programs/on-call.html.

[3] D. S. Callaway and I. A. Hiskens, "Achieving controllability of electric loads," *Proceedings of the IEEE*, vol. 99, no. 1, pp. 184–199, Jan 2011.

[4] J. L. Mathieu, S. Koch, and D. S. Callaway, "State estimation and control of electric loads to manage real-time energy imbalance," *IEEE Transactions on Power Systems*, vol. 28, no. 1, pp. 430–440, Feb 2013.

[5] Y. Chen, A. Busic, and S. Meyn, "Estimation and control of quality of service in demand dispatch," *IEEE Transactions on Smart Grid*, vol. 9, no. 5, pp. 5348–5356, Sep. 2018.

[6] Y. Chen, M. U. Hashmi, J. Mathias, A. Bušić, and S. Meyn, *Distributed Control Design for Balancing the Grid Using Flexible Loads*. New York, NY: Springer New York, 2018, pp. 383–411. [Online]. Available: https://doi.org/10.1007/978-1-4939-7822-9_16

[7] H. Hao, Y. Lin, A. S. Kowli, P. Barooah, and S. Meyn, "Ancillary service to the grid through control of fans in commercial building hvac systems," *IEEE Transactions on Smart Grid*, vol. 5, no. 4, pp. 2066–2074, July 2014.

[8] M. Almassalkhi, J. Frolik, and P. Hines, "Packetized energy management: Asynchronous and anonymous coordination of thermostatically controlled loads," in *2017 American Control Conference (ACC)*, May 2017, pp. 1431–1437.

[9] S. P. Meyn, P. Barooah, A. Busic, Y. Chen, and J. Ehren, "Ancillary service to the grid using intelligent deferrable loads," *IEEE Transactions on Automatic Control*, vol. 60, no. 11, pp. 2847–2862, Nov 2015.

[10] Z. Ma, D. Callaway, and I. Hiskens, "Decentralized charging control for large populations of plug-in electric vehicles: Application of the nash certainty equivalence principle," in *2010 IEEE International Conference on Control Applications*, Sep. 2010, pp. 191–195.

[11] Y. Chen, A. Busic, and S. Meyn, "Individual risk in mean field control with application to automated demand response," in *53rd IEEE Conference on Decision and Control*, Dec 2014, pp. 6425–6432.

[12] Y. Chen, A. Busic, and S. P. Meyn, "State estimation for the individual and the population in mean field control with application to demand dispatch," *IEEE Transactions on Automatic Control*, vol. 62, no. 3, pp. 1138–1149, March 2017.

[13] D. S. Callaway, "Tapping the energy storage potential in electric loads to deliver load following and regulation, with application to wind energy," *Energy Conversion and Management*, vol. 50, no. 5, pp. 1389 – 1400, 2009. [Online]. Available: http://www.sciencedirect.com/science/article/pii/S0196890408004780

[14] B. Bamieh and L. Giarre, "Identification of linear parameter varying models," *International Journal of Robust and Nonlinear Control*, vol. 12, no. 9, pp. 841–853, 2002. [Online]. Available: http://dx.doi.org/10.1002/rnc.706

[15] S. Shalev-Shwartz and S. Ben-David, *Feature Selection and Generation*. Cambridge University Press, 2014, p. 309–322.

[16] G. F. Franklin, J. D. Powell, and A. Emami-Naeini, *Feedback Control of Dynamic Systems*, 7th ed. Upper Saddle River, NJ, USA: Prentice Hall Press, 2014.

[17] Distribution System Analysis Subcommittee, IEEE Power Engineering Society, "IEEE 37 Node Test Feeder." [Online]. Available: http://sites.ieee.org/pes-testfeeders/resources/

[18] "BPA balancing authority load and total wind, hydro, and thermal generation (website)," https://transmission.bpa.gov/business/operations/Wind/baltwg.aspx.

Appendix I
Linear Representation of the LPV Model

We represent the LPV model (11) in the following form

$$\hat{y}_t = \text{trace}(\Theta^T \Psi_{t-1}) \tag{17}$$

with

$$\Theta^T := \begin{bmatrix} a_{1,0} & \dots & a_{m,0} & b_{1,0} & \dots & b_{n,0} \\ \vdots & \vdots & \vdots & \vdots & \dots & \vdots \\ a_{1,v} & \dots & a_{m,v} & b_{1,v} & \dots & b_{n,v} \end{bmatrix}$$

$$\Psi_{t-1} := \begin{bmatrix} -y_{t-1} \\ \vdots \\ -y_{t-m} \\ u_{t-1} \\ \vdots \\ u_{t-n} \end{bmatrix} \begin{bmatrix} 1 & p_1 & \dots & p_v \end{bmatrix}.$$

We introduce a vectorization operator vec$(\cdot)$ that transforms a matrix to a column vector by stacking matrix columns, e.g.,

$$\text{vec}\left(\begin{bmatrix} a_{1,1} & a_{1,2} \\ a_{2,1} & a_{2,2} \end{bmatrix} \right) = \begin{bmatrix} a_{1,1} & a_{2,1} & a_{1,2} & a_{2,2} \end{bmatrix}^T$$

Letting $\theta = \text{vec}(\Theta)$ and $\phi_{t-1} = \text{vec}(\Psi_{t-1})$, we obtain (12).